

Surveys of Returned ISS Hardware for MMOD Impacts

Hyde, J.L.⁽¹⁾, Christiansen, E.L.⁽²⁾, Lear, D.M.⁽³⁾, Nagy, K.⁽⁴⁾, Berger, E.L.⁽⁵⁾

⁽¹⁾ Barrios Technology, NASA/JSC, Mail Code XI4, Houston, Texas, 77058, USA, Email: james.l.hyde@nasa.gov

⁽²⁾ NASA/JSC, Mail Code XI4, Houston, Texas, 77058, USA, Email: eric.l.christiansen@nasa.gov

⁽³⁾ NASA/JSC, Mail Code XI4, Houston, Texas, 77058, USA, Email: dana.m.lear@nasa.gov

⁽⁴⁾ NASA/JSC, Mail Code ES2, Houston, Texas, 77058, USA, Email: kornel.nagy-1@nasa.gov

⁽⁵⁾ Jacobs Technology, NASA/JSC, Mail Code XI3, Houston, Texas, 77058, USA, Email: eve.l.berger@nasa.gov

ABSTRACT

Since February 2001, the Hypervelocity Impact Technology (HVIT) group at the Johnson Space Center (JSC) in Houston has performed 35 post-flight inspections on space exposed hardware returned from the International Space Station (ISS). Data on 1,188 observations of micrometeoroid and orbital debris (MMOD) damage have been collected from these inspections. Survey documentation typically includes impact feature location and size measurements as well as microscopic photography (25-200x). Sampling of impacts sites for projectile residue was performed for the largest features. Results of energy dispersive X-ray spectroscopic analysis to discern impactor source are included in the database when available. This paper will focus on two inspections, the Pressurized Mating Adapter 2 (PMA-2) cover returned in 2015 after 1.6 years exposure with 26 observed impact features, and two Airlock shield panels returned in 2010 after 8.75 years exposure with 58 MMOD impacts. Feature sizes from the observed data are compared to predictions using the Bumper 3 risk assessment code.

1 PMA-2 COVER

Two of the three Pressurized Mating Adapters (PMAs) on the International Space Station (ISS) are utilized for visiting vehicles. In recent years both PMA-2 and PMA-3 had temporary covers installed over the docking port to provide thermal control and MMOD protection. The covers were constructed with Beta cloth outer layers and internal layers of ballistic fabric. The PMA-2 cover (Fig. 1) was installed on the forward facing docking port during US extravehicular activity (EVA) #22 on July 9, 2013 and removed during US EVA #30 on February 25, 2015 [1]. The cover was returned May 21, 2015 on the SpaceX CRS-6 mission and a post flight MMOD inspection was performed by NASA, Jacobs and Boeing personnel at the JSC HVIT facility on March 16, 2016.

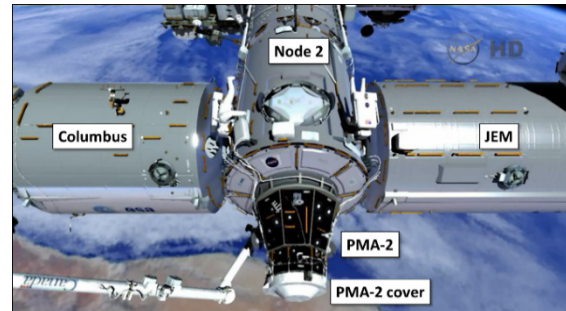


Figure 1. Location of PMA-2 cover

2 PMA-2 INSPECTION RESULTS

Fig. 2 shows the inspection of the PMA-2 cover at JSC. The circular blanket was approximately 2 meters in diameter with a 0.20 mm thick beta cloth (silica fiber) outer cover. Also inspected were nine beta cloth straps that were used to hold the cover in place on the PMA. The inspection was performed in three steps. An initial screening was performed on all space exposed surfaces with 15X handheld magnifiers, with 34 areas of interest marked for further study. In the second step each area of interest was examined with a handheld 25X-200X microscope enabling a more detailed characterization. 26 sites were observed with distinct hypervelocity impact features and 8 sites were judged to be non-MMOD. Fig. 3 shows feature #1 from Tab.1 as typical MMOD impact damage observed during the inspection. The final inspection step involved a boom mounted digital microscope that allowed precise measurements of the entry hole.



Figure 2. PMA-2 cover inspection

Damage sizes on the beta cloth outer surface of the cover and the hold-down straps ranged from just over 1mm to 0.13mm in diameter.

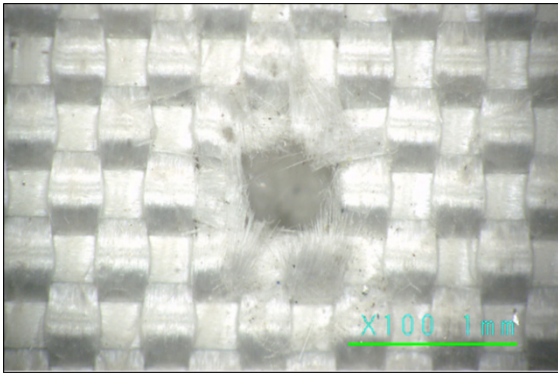


Figure 3. Typical impact damage on PMA-2 cover

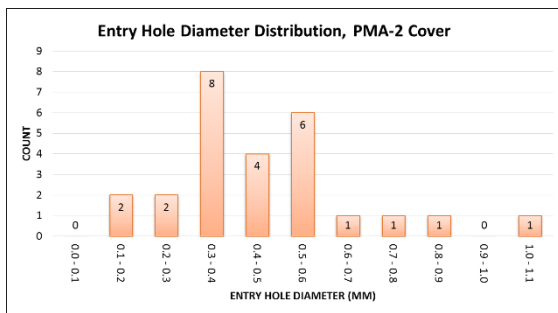


Figure 4. Distribution of PMA-2 entry hole sizes

An equivalent circular hole size was determined from the maximum (D1) diameter and the hole dimension in the orthogonal direction to the maximum direction (D2).

$$D_{hole} = (D1 * D2)^{0.5} \quad (1)$$

Eq. 1 results in a circular area with the same area as the measured hole assuming elliptical geometry for the hole. Calculated entry hole diameters are provided in Tab. 1. It can be seen in the distribution of entry hole diameters (Fig. 4) that feature sizes in the 0.3 to 0.6 mm range were the most common. The mean value of the 26 observations was 0.45 mm.

Table 1. Damage sizes on PMA-2 cover

Feature #	D1 (mm)	D2 (mm)	D _{hole} (mm)	d _p (mm)
1	0.62	0.59	0.60	0.26
2	1.19	0.85	1.01	0.44
3	0.50	0.44	0.47	0.20
4	0.60	0.58	0.59	0.26
5	0.33	0.31	0.32	0.14
6	0.41	0.29	0.34	0.15
7	0.55	0.47	0.51	0.22
8	0.60	0.53	0.56	0.25
9	0.37	0.37	0.37	0.16
10	0.93	0.69	0.80	0.35

11	0.44	0.38	0.41	0.18
12	0.73	0.44	0.57	0.25
13	0.75	0.71	0.73	0.32
14	0.40	0.25	0.32	0.14
15	0.41	0.38	0.39	0.17
16	0.33	0.30	0.31	0.14
17	0.33	0.31	0.32	0.14
18	0.49	0.35	0.41	0.18
19	0.27	0.23	0.25	0.11
20	0.44	0.43	0.43	0.19
21	0.19	0.12	0.15	0.07
22	0.31	0.21	0.26	0.11
23	0.61	0.57	0.59	0.26
24	0.37	0.35	0.36	0.16
25	0.58	0.46	0.52	0.22
26	0.14	0.12	0.13	0.06
Mean	0.50	0.41	0.45	0.20
Max	1.19	0.85	1.01	0.44
Min	0.14	0.12	0.13	0.06

3 ANALYSIS of PMA-2 DAMAGE SITES

3.1 Sampling

Six intact impact features (#1, 2, 10, 12, 13 and 24) were extracted with a hammer and punch. The samples were stored in cases that preserved the orientation of the individual blanket layers.

3.2 SEM/EDS Results

SEM/EDS analysis results are summarized in Tab. 2. Four of the six samples yielded results that indicate high density orbital debris as the source.

Table 2. PMA-2 Cover SEM/EDS Results

#	Hole Diameter (mm)	Impactor Type/ Major Constituent	Possible Impactor
1	0.60	OD: Steel, ZnS, FeO, Ti	Steel
2	1.01	OD: Steel, Nickel-Oxide	Steel
10	0.80	OD: Steel, Iron-oxide	Steel
12	0.57	MM: Ca, Mg, Fe, S, O	Chondrite
13	0.73	MM: Fe, Ni, S	metal/ sulfide-rich MM
24	0.36	OD: Steel, Iron-oxide, Ti	Steel

An example of the scanning electron microscopy used to determine the nature of the impactors on the PMA-2 cover is provided for impact #13, observed on one of the tie down straps. The impact area is backlit in Fig. 5, highlighting the extent of the subsurface damage. The impact event melted both the projectile and the beta cloth target (Figs. 6-7). Analysis by scanning electron microscope indicated this damage was due to a micrometeoroid impactor rich in iron, nickel and sulfur.

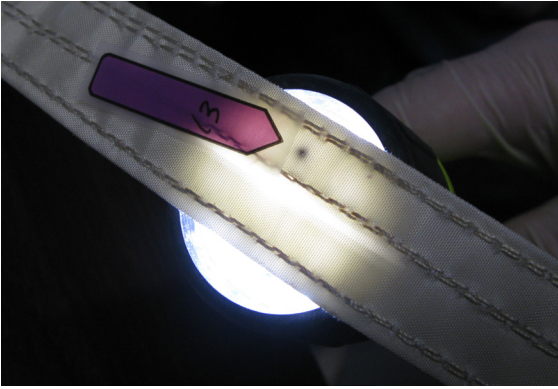


Figure 5. Impact in PMA-2 cover tie down strap

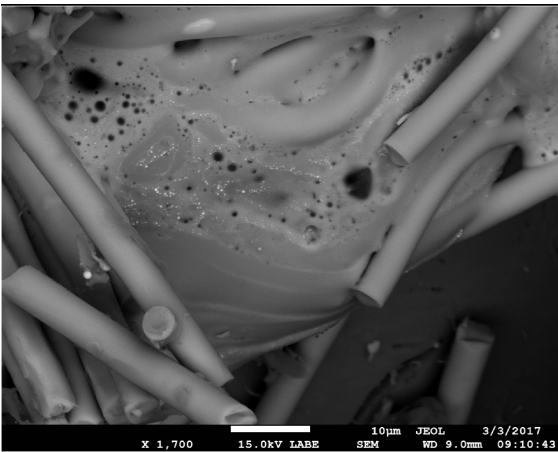


Figure 6. Impactor melt flow around beta cloth fibers

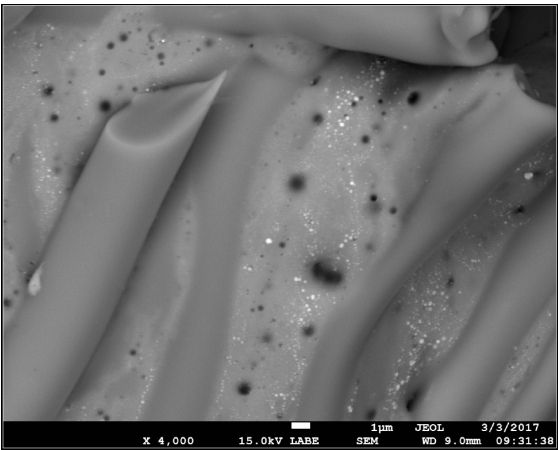


Figure 7. Close-up image of impactor melt droplets

4 PREDICTIONS OF PMA-2 COVER DAMAGE WITH BUMPER 3

4.1 Particle Size Estimate

A damage equation for beta-cloth was developed based on hypervelocity impact data for small particles (<0.4 mm diameter) [2]. Eq. 2 relates the clear-hole diameter (D_{hole}) in the beta cloth to the projectile diameter (d_p).

$$D_{hole} = 2.3d_p \quad (2)$$

No correlation with projectile velocity, angle or density was attempted due to lack of data. Estimated particle diameter for each observed feature is shown in the “ d_p ” column of Tab. 1.

4.2 Bumper 3 Inputs

The analysis procedure in Bumper 3 [6] involved calculating the expected number of MM and OD impacts from selected particle diameters in Tab. 1. The standalone finite element representation of the PMA-2 cover used as the input geometry in Bumper 3 is shown in the right hand side of Fig. 8.

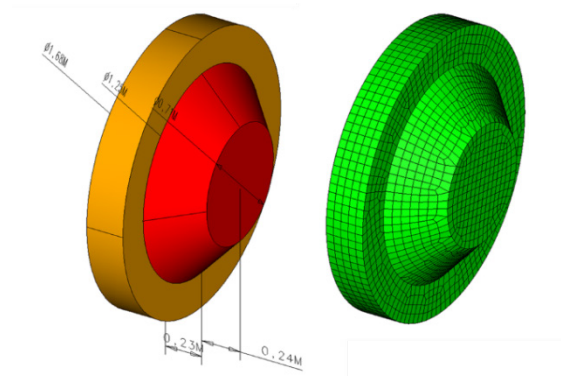


Figure 8. PMA-2 cover surface geometry and FE model

For each year of the assessment (2013 through 2015) the Orbital Debris Program Office (ODPO) at JSC produced ORDEM 3.0 data files for the assessment [3] using time-averaged altitude data provided by HVIT, shown in Tab. 3. The MEM-R2 environment model [4], was used to produce the “MEMR2_LEO_ISS.out” data file at 400 kilometer altitude and 51.6° inclination.

Table 3. PMA-2 cover exposure time and altitude

Start Date	End Date	Days	Years	Altitude (km)
7/9/13	1/1/14	176	0.482	413.6
1/1/14	1/1/15	365	1.000	414.5
1/1/15	2/25/15	55	0.151	402.1
Total		596	1.633	

4.3 Bumper 3 Results

Predictions from Bumper 3 for the number of MEM-R2 and ORDEM 3.0 impacts are provided in Tab. 4 for six representative particle diameters. Using Eq. 2, equivalent hole diameters are also given. The lower bound on the predictions was set at 0.0125 cm due to the fact that diameters below that are not available in the release version of MEM-R2. The expected number of

ORDEM 3.0 impacts for each particle diameter were assessed for years 2013, 2014 and 2015 with the results for 2013 and 2015 scaled by the durations shown in Tab. 3. One year MEM-R2 impact predictions for the six diameters were scaled by the 1.633 year total exposure time. Using the Regression data analysis tool in Excel, coefficients for continuous curves of expected values were derived from the Bumper 3 predictions.

Table 4. Bumper 3 predictions for PMA-2 damage

Hole Diam (cm)	Particle Diam (cm)	MEM R2	ORDEM 3.0	MEMR2 + ORDEM3
0.0288	0.0125	16.89	14.60	31.49
0.0460	0.020	4.40	3.87	8.27
0.0920	0.040	0.46	0.68	1.14
0.1380	0.060	0.11	0.30	0.40
0.1840	0.080	0.04	0.15	0.19
0.2300	0.100	0.02	0.08	0.10

Fig. 9 compares the observed entry hole diameters on the PMA-2 cover with Bumper 3 predictions for the expected number of impacts from ORDEM 3.0 and MEMR2. Observations below 0.03 cm show typical roll-off at the small end of MMOD inspection data sets, due to the difficulty in finding small impact features (i.e., sensor/observation limitations).

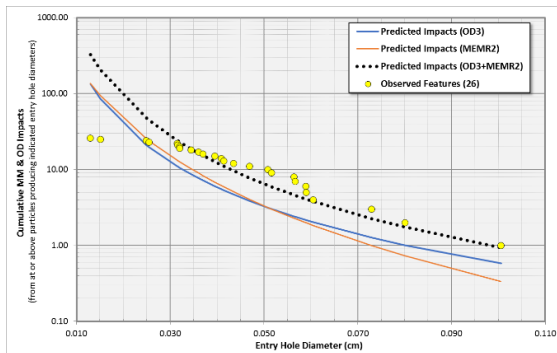


Figure 9. Comparison of 26 estimated particle sizes causing observed damage on the PMA-2 cover and Bumper 3 predictions

5 AIRLOCK SHIELD PANELS

The Quest airlock was launched on the Space Shuttle Atlantis STS-104 mission and installed on the starboard side of Node 1 during ISS assembly flight 7A in July 2001. At the same time two oxygen and two nitrogen High-Pressure Gas Tanks (HPGT) were installed on the airlock. In November 2009, the STS-129 Shuttle mission delivered a fifth HPGT as part of the ULF-3 assembly flight. To make way for the new HPGT installation, two airlock shield panels were removed, covered with an insulation blanket and stored on an external logistics pallet until they were returned on the 19A assembly flight on April 2010 after nearly 8.75

years of exposure time. The post flight MMOD inspection was performed by NASA and Jacobs personnel on January 7, 2011 in JSC Building 13. Fig. 10 shows the zenith side of the airlock with the removed shield panels highlighted.

6 AIRLOCK INSPECTION RESULTS

The airlock shield panels are made of aluminum 6061-T6 and are each 1.3 m long, 0.84 m wide and 0.2 cm thick. The survey of these panels was limited to a visual inspection with additional characterization by handheld digital microscope. Craters less than 0.25 mm diameter were not recorded. The inspection measured the “inside diameter” of the crater, recorded at the original height of the panel surface. A total of 58 craters were observed, 34 on the outboard panel and 24 on the inboard. The inspected shield panels can be seen in Fig. 11 with the 58 regions of interest flagged (colored arrows). 56 of the 58 observed craters were nearly circular, with only two elliptical craters recorded. The largest circular impact crater (Fig. 12) measured 1.8 mm in diameter.

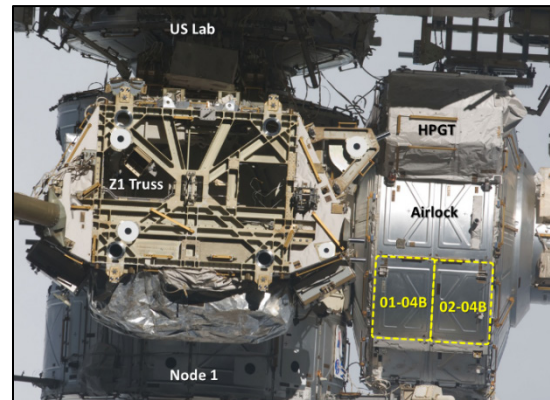


Figure 10. Location of removed airlock shields

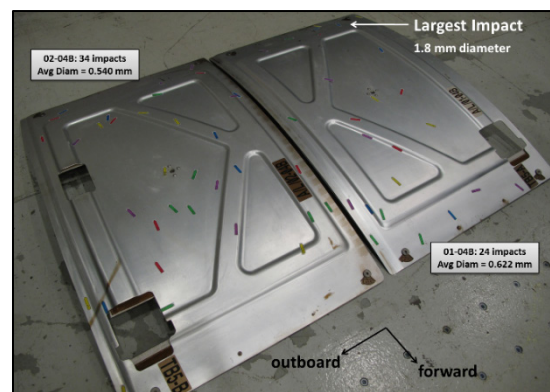


Figure 11. Inspection results on airlock shields

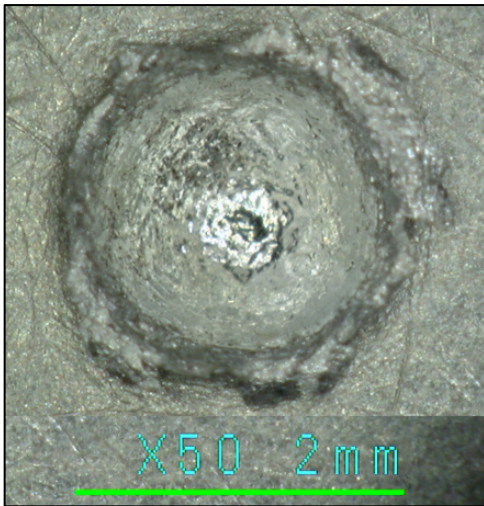


Figure 12. 1.8 mm impact crater on airlock panel

This impact produced a 2 mm diameter bulge on the backside of the 2.03 mm shield panel. An elliptical crater measuring 2.4 x 0.9 mm (Fig. 13) was observed on the same panel.

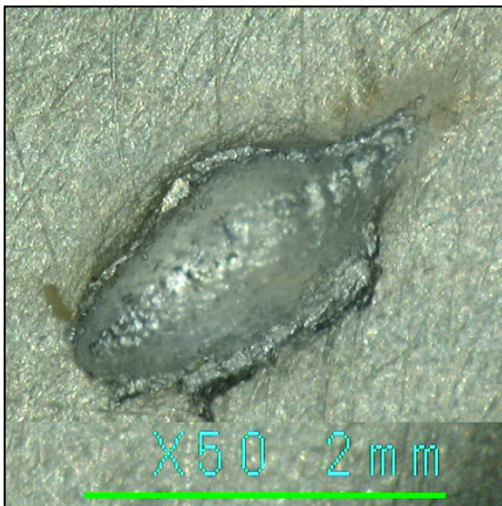


Figure 13. 2.4 x 0.9 mm impact crater on airlock panel

An equivalent circular crater size was calculated from measured dimensions using Eq. 1 and the crater diameter distribution is given in Fig. 14.

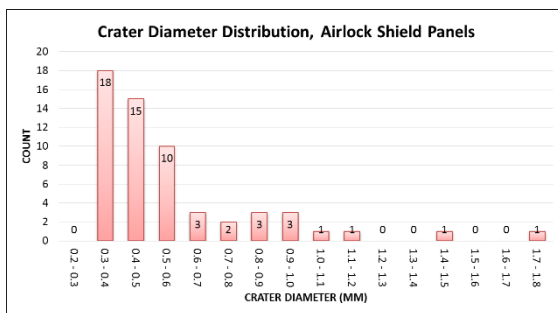


Figure 14. Distribution of airlock crater diameters

7 ANALYSIS OF AIRLOCK DAMAGE SITES

7.1 Sampling

Since intact extraction of entire craters was not permitted by the hardware owners, samples were collected at nine damage sites. In Figs. 12 and 13 the raised crater lips typically present in aluminium target impact can be seen. The sampling technique for the airlock shield involved removing portions of the crater lip material and retrieving small fragments scraped from the crater bottom. Red dots in Figs. 15 and 16 indicate the locations of the sampled craters.

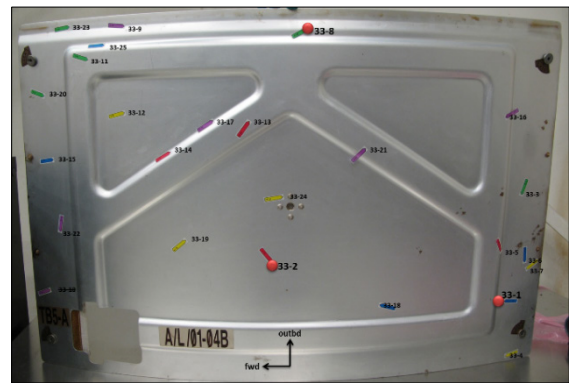


Figure 15. 24 craters on airlock shield 01-04B, sampled craters highlighted with red circles

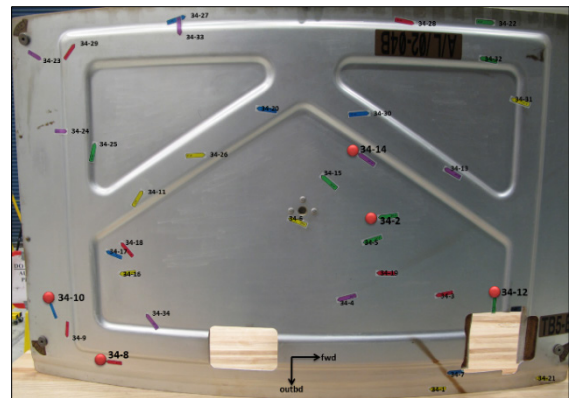


Figure 16. 34 craters on airlock shield 02-04B, sampled craters highlighted with red circles

7.2 SEM/EDS Results

SEM/EDS analysis results are summarized in Tab. 5. Eight of the nine samples yielded results that indicate orbital debris as the source.

Table 5. Airlock SEM/EDS Results

Sample	Crater Diameter (mm)	Impactor Type/Major Constituent	Possible Impactor
33-1	1.78	OD: SiO	Silica
33-2	1.06	OD: CF, Si, SiO	PTFE, Silica

33-8	1.48	OD: Fe, SiO, Pb, Cr, Ni, Co	Silica, paint, metal alloys
33-21	0.73	unknown	--
34-2	1.17	OD: CF, Fe	PTFE
34-8	0.42	OD: CF, K, Ca, Ti, SiO	PTFE, Silica
34-10	0.81	OD: SiO, Fe, Cu, Zn	Silica
34-11	0.91	OD: SiO, BaS, Cu, Zn	Silica, paint
34-14	0.85	OD: CF	PTFE

Crater 33-1 is shown in Fig. 12. An extracted sample from the crater with the associated SEM image and spectra are given in Fig. 17. This sample along with many others appeared to have silica melted into the aluminium.

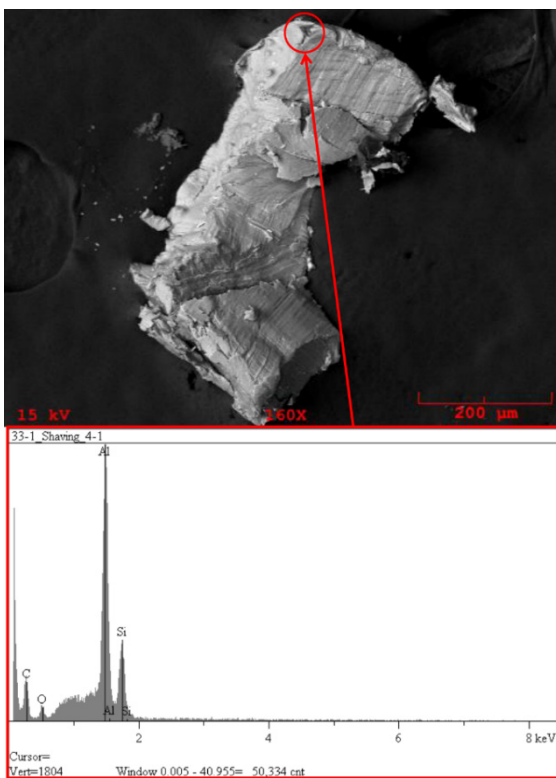


Figure 17. SEM results of sample from crater 33-1 indicate trace silica melt in the aluminum

8 AIRLOCK DAMAGE PREDICTIONS

8.1 Feature Size Estimate

Tab. 5 provides a listing of the crater diameters observed on the airlock shield panel. Effective crater diameter (D_c) was calculated using Eq. 1. Assuming that crater depth is $\frac{1}{2}$ crater diameter, Bumper 3 was used to estimate the expected number of five representative crater depth cases using the Cour-Palais single wall equation [5] on a 6061-T6 aluminium wall.

Table 6. Airlock shield crater diameters. Sampled impact sites are highlighted

Impact #	D1 (mm)	D2 (mm)	D_c (mm)
34-1	0.5	0.6	0.57
34-2	1.3	1.1	1.17
34-3	0.4	0.5	0.45
34-4	0.5	0.5	0.54
34-5	0.5	0.5	0.54
34-6	0.6	0.6	0.58
34-7	0.5	0.5	0.47
34-8	0.4	0.4	0.42
34-9	0.5	0.5	0.51
34-10	0.8	0.8	0.81
34-11	0.9	0.9	0.91
34-12	0.4	0.4	0.45
34-13	0.6	0.6	0.60
34-14	0.9	0.8	0.85
34-15	1.0	1.0	0.97
34-16	0.4	0.4	0.36
34-17	0.4	0.4	0.44
34-18	0.4	0.4	0.39
34-19	0.4	0.4	0.36
34-20	0.6	0.6	0.57
34-21	0.5	0.5	0.50
34-22	0.4	0.4	0.38
34-23	0.6	0.5	0.57
34-24	0.4	0.4	0.39
34-25	0.4	0.4	0.41
34-26	0.4	0.4	0.38
34-27	0.5	0.4	0.45
34-28	1.0	0.9	0.95
34-29	0.5	0.4	0.43
34-30	0.4	0.4	0.38
34-31	0.4	0.4	0.36
34-32	0.4	0.4	0.36
34-33	0.4	0.4	0.43
34-34	0.4	0.4	0.38
33-1	1.8	1.8	1.78
33-2	1.0	1.1	1.06
33-3	0.6	0.5	0.57
33-4	0.8	0.7	0.72
33-5	0.6	0.6	0.61
33-6	0.4	0.4	0.43
33-7	0.4	0.4	0.38
33-8	0.9	2.4	1.48
33-9	0.6	0.6	0.58
33-11	0.5	0.5	0.48
33-12	0.7	0.6	0.66
33-13	0.5	0.4	0.45
33-14	0.5	0.5	0.47
33-15	0.9	0.8	0.84
33-16	0.4	0.4	0.36
33-17	0.4	0.4	0.37
33-18	0.4	0.4	0.38
33-19	0.4	0.4	0.37
33-20	0.5	0.5	0.51
33-21	0.4	1.4	0.73
33-22	0.3	0.3	0.33
33-23	0.3	0.3	0.32
33-24	0.3	0.3	0.31
33-25	0.4	0.5	0.42
Mean			0.568
Max			1.781
Min			0.311

8.2 Bumper 3 Inputs

The analysis was performed against a 1.98 m² finite element mesh area on the equipment lock region of the airlock. The region is highlighted in Fig. 18.

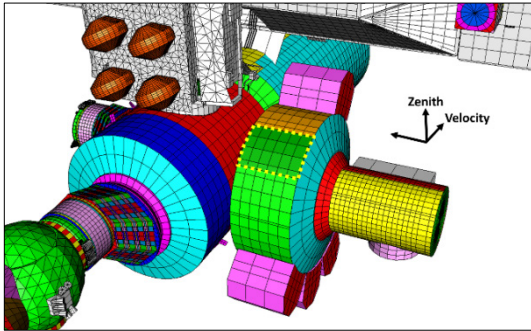


Figure 18. Airlock shield FEM

For each year of the assessment (2001 through 2010) ORDEM 3.0 data files using time-averaged altitude data were provided by the JSC Orbital Debris Program Office (Tab. 7). The “MEMR2_LEO_ISS.out” data file distributed with Bumper 3 was used in the calculations.

Table 7. Altitude, exposure time and relevant events

Year	Altitude (km)	Time (year)	Event
2001	382.68	0.466	07/14/01: Airlock install
2002	390.04	1.0	
2003	384.61	1.0	
2004	361.66	1.0	
2005	352.54	1.0	
2006	342.20	1.0	
2007	337.55	1.0	10/27/07: P6 moved from Z1 to P5
2008	345.41	1.0	
2009	348.55	1.0	11/23/09: airlock shields to ESP-2
2010	349.40	0.282	04/13/10: shields retrieved from ESP-2
Total		8.753	

8.3 Bumper 3 Results

Predictions from Bumper 3 for the number of craters from MEM-R2 and ORDEM 3.0 are provided in Tab.8 for five representative depth values. Individual ORDEM 3.0 assessments were performed for each year from 2001 through 2010 with the results for 2001 and 2010 scaled by the durations shown in Tab. 7. MEM-R2 results with a one year exposure were scaled by the total exposure time of 8.753 years.

Table 8. Bumper 3 predictions for Airlock crater depths

Crater Depth (cm)	Crater Diameter (cm)	MEM R2	ORDEM 3.0	MMOD TOTAL
0.02	0.04	26.955	0.026	26.980

0.04	0.08	4.726	0.006	4.732
0.06	0.12	1.467	0.003	1.470
0.08	0.16	0.605	0.002	0.607
0.10	0.20	0.297	0.001	0.298

All 58 observed craters are compared with ORDEM 3 and MEMR2 in Fig. 19. Bumper 3 predicts nearly all ($\geq 99.7\%$) of the craters are from micrometeoroids. The predicted number of MMOD impacts was higher than observed. The explanation for this is that there were more orbital debris impacts observed and very little orbital debris was predicted to hit these panels because their location on ISS should have prevented orbital debris from impacting them. We believe the likely explanation for this discrepancy is that the orbital debris found on the airlock panels was due to secondary debris (ejecta or penetration products) produced by MMOD impacts on the ISS radiators and solar arrays. The composition of the OD particles determined by SEM analysis supports this hypothesis, with many of the craters containing silica (potentially from solar arrays) and paint (possibly from radiators).

8 of the 9 samples that were analyzed produced indications of orbital debris. The 8 observed craters attributed to orbital debris are compared to ORDEM 3 predictions in Fig. 20. The predicted number of craters from orbital debris is very small compared to micrometeoroids due to the orientation of the shield panels on the zenith/aft facing region of the airlock.

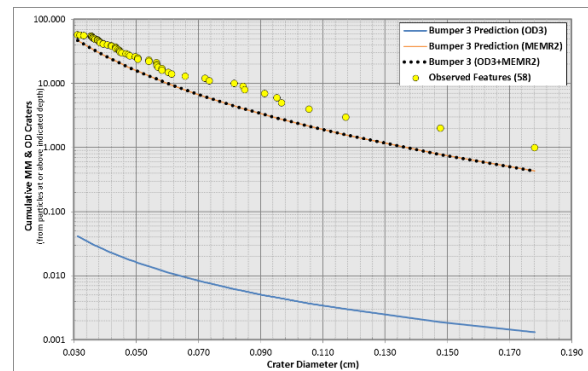


Figure 19. Comparison of Bumper 3 predictions using ORDEM 3 and MEMR2 to all observed MMOD impacts

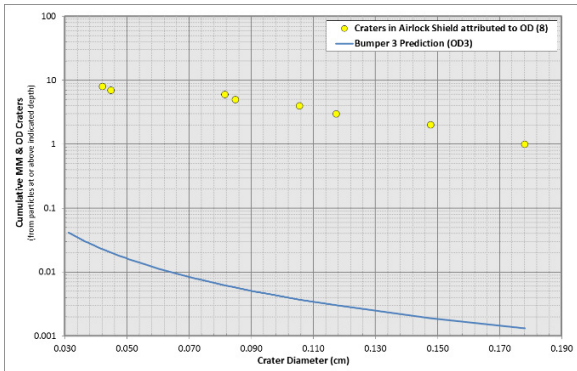


Figure 20. Comparison of Bumper 3 predictions using ORDEM 3 to impacts attributed to orbital debris

9 CONCLUSIONS

The damage found in post-flight inspection of the PMA cover and the returned airlock bumper panels was generally consistent with Bumper code predictions using the ORDEM 3.0 debris model and MEM-R2 meteoroid model. An excess of orbital debris damage was observed on the airlock bumper panels compared to predictions, although this discrepancy is likely the result of secondary debris impacts. Fig. 21 shows the ISS configuration for a majority of the time the airlock panels were exposed to MMOD. The airlock bumper panels lie in close proximity to the solar array wings on the P6 truss. The silica rich impact sites on the airlock panels could be a product of secondaries from the solar array panels, either front side ejecta from the initial impact or back side penetration products. Painted radiator surfaces are also near the airlock shield panels, and secondaries from these surfaces could account for the paint detected by SEM in some of the airlock craters.

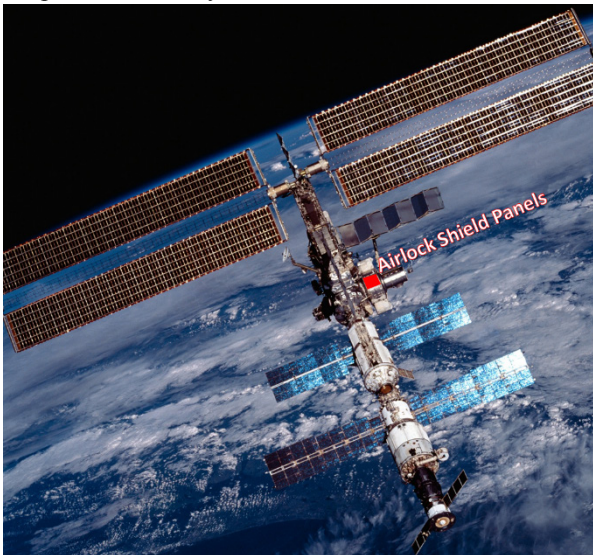


Figure 21. Airlock on ISS after 7A mission

10 REFERENCES

1. Flight Operations Directorate EVA History Wiki, https://wiki.jsc.nasa.gov/eva/index.php/EVA_History
2. Christiansen, E.L. (2017). Personnel communication on ballistic limit equations for beta cloth.
3. Stansbery, E.G. (2014). NASA Orbital Debris Engineering Model ORDEM 3.0 - User's Guide. NASA/TP-2014-217370.
4. Moorhead, A.V. (2015). NASA Meteoroid Engineering Model Release 2.0. NASA/TM-2015-218214
5. Christiansen, E.L. (1993). Design and Performance Equations for Advanced Meteoroid and Debris Shields. *Int. J. Impact Eng.*, 14:145–15
6. Bjorkman, M. D. (2014). Bumper 3 Software User Manual. NASA/TM-2014-218559